http://dx.doi.org/10.11142/jicems.2013.2.3.349

Optimisation of an inductive power transfer structure

Romain Besuchet *, Christophe Auvigne *, Dan Shi *, Christophe Winter *, Yoan Civet *, and Yves Perriard *

Abstract – This paper presents the multi-objective optimisation of an Inductive Coupled Power Transfer (ICPT) device. A setup as complicated as the one at hand in this paper is extremely hard to model analytically. To acquire some knowledge about the influence of the geometric factors, a sensitivity analysis is first performed using design of experiment (DoE) and finite-element modelling (FEM). It allows validating that the choice of the free factors is relevant. This being done, the optimisation itself is performed using a genetic algorithm (GA), with two objectives and a strict functioning constraint.

Keywords: Design of experiment, Genetic algorithm, Inductive coupled power transfer, Optimisation, Sensitivity analysis

1. Introduction

Contactless power transfer consists in transferring electric power from a power supply to a mobile load without any physical link. Although several technologies exist for this purpose, only Inductive Coupled Power Transfer (ICPT) is studied in this paper. The latter is used in a lot of different applications. For low-power transfer (< 100W), it is widely used for desktop peripherals supply and cellphone chargers [1]–[3]. For medical purpose, contactless power transmission is used to supply devices inside the patient's body, isolating it from its environment [4].

For mid-range and high-power transfer applications, electric vehicle supplies and battery chargers are widely investigated fields. Indeed, it increases security removing the need to plug any electric cable. Also, it allows uninterrupted power supply, even while the vehicle is in motion [5]–[7].

This paper focuses on the design of a coreless transformer for a small electric vehicle. Specifically, the coils and the environment are investigated. Since iron parts are present under the vehicle, a shielding is placed in order to reduce the Joule losses induced by Eddy currents in the conductive parts. Depending on the specifications of the transformer, various shielding configurations can be used [8]–[10]. In order to increase the magnetic coupling between the primary and secondary parts (also called pads), several coils can be placed in different configurations and supplied with different phases [11], [12].

The studied topology is presented in Fig. 1. The transformer is composed of two identical power parts. Each one contains a planar circular coil, a ferrite plate to direct the magnetic field. An aluminium backplate is placed under the ferrite to stop the leakage flux by eddy currents. Finally, a copper ring is placed in order to reduce lateral leakage field in order to be compliant with the European recommendations [13].

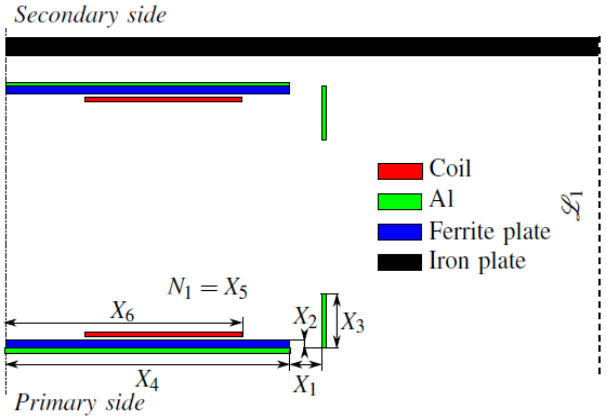

Fig. 1. Geometry of the transformer and its shielding (axisymmetric cross-section)

The aim of this paper is to optimise this structure. The basics of ICPT are first introduced. Then, a sensitivity analysis of the system is performed using Design of Experiment (DoE) and Finite Element Modelling (FEM). This sensitivity analysis is done to verify the importance of the geometric factors on the performances of the system.

* Integrated Actuators Laboratory (LAI), Institute of Microengineering (IMT), École polytechnique fédérale de Lausanne (EPFL), Switzerland
Received 14 July 2013; Accepted 22 August 2013

Finally, a global optimisation of the transformer's performance using Genetic Algorithm (GA) is done. The two objectives functions are minimising the magnetic losses and the maximum radiated magnetic field along the line *L1*.

2. ICPT Basics

The conversion chain of a typical ICPT is illustrated in Fig. 2. The DC power supply is converted into an AC one through a resonant power inverter. At the secondary side, the AC induced voltage is rectified to obtain a DC voltage to supply the load.

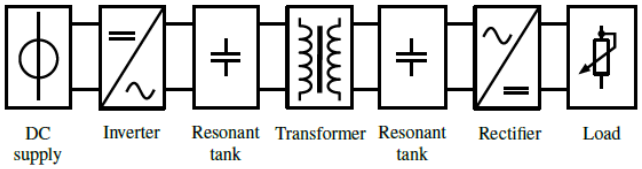

Fig. 2. Overview of the ICPT conversion chain

Due to the low magnetic coupling factor of the transformer, it is capacitive compensated in order to increase its power factor, power transfer capability and efficiency [14]. According to [15], the compensation capacitances can be placed either in series or in parallel with the coils, leading to four main topologies. The 'series-series' (SS) topology is chosen. Its electric equivalent circuit is shown in Fig. 3 U_{in} is the input voltage, U_L the load voltage, ω the supply frequency, I_1 and I_2 the primary and secondary currents respectively, R_1, R_2, L_1, L_2, C_1, C_2 are the resistance, self-inductance and compensation capacitance of the primary and secondary sides. This topology has some advantages. First of all, it behaves like a current source supplying the load if the transformer is driven with a constant voltage U_{in}. This allows to directly connect the battery to the rectifier without any additional power converter. Moreover, unlike the others topologies, the values of the compensation capacitances C_1 and C_2 are independent of the coupling factor of the transformer and the load value. The capacitances C_1 and C_2 are evaluated in (1), where ω_0 is the resonant pulsation.

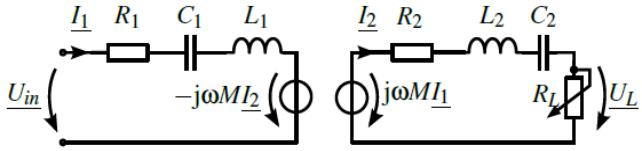

Fig. 3. Electric equivalent circuit of the SS topology

Neglecting the serial resistances of the coils R_1 and R_2 regarding R_L and $\omega_0 M$, the relationship between the mutual inductance M, the load current I_2 and the supply voltage U_{in} is given in (2).

$$\begin{cases} C_1 = \dfrac{1}{\omega_0^2 L_1} \\ C_2 = \dfrac{1}{\omega_0^2 L_2} \end{cases} \quad (1)$$

$$M = \frac{U_{in}}{I_2 \omega_0} \quad (2)$$

In this paper, the load power is set to P_L = 500 W, the load voltage is set to U_L = 40 V, the supply voltage is set to U_{in} = 50 V and the pulsation is set to $\omega_0 = 2 \cdot \pi \cdot 50000$ rad s^{-1}.

3. ICPT Basics

The target of the sensitivity analysis is to acquire knowledge about how much effect each free factor has on some output of interest. The analysis is performed using DoE, which is a statistical technique based on experiments. In particular, it provides powerful tools for empirical modelling and screening. The major idea of this technique is to smartly select the group of experiments to perform, for a given number of free factors. A group of experiments is called an *experimental design*. Obviously, results, later on called *responses*, cannot be known before performing the experiments but several conclusions can be deduced simply based on the experimental plan. Particularly, for a given type of empirical model, the efficiency of an experimental design for identifying the model parameters can be deduced mathematically. This will of course be used to define the experiments.

3.1. Experiments

The experiments conducted here consist in evaluating the mutual inductance of a transformer depending on the value of its geometric parameters, as well as estimating its magnetic efficiency for a given load power. The first response is used to analyse the effects of the optimization constraints. The second one does not exactly correspond to the objectives of the optimisation for consistency reasons. Indeed, comparing the losses in systems can only be done for systems having the same output power, which is not the case when the operating conditions are not fixed. Similarly, it would be irrelevant to compare the emitted magnetic field in the conditions.

The experiments are not carried out physically, but using FEM. Each experiment consists in one simulation of the

model shown in Fig. 1, performed with the commercial software FLUX2D. The two responses for each experiment can be calculated together with only one FEM solving, which limits the computation time.

3.2. Empirical models and full factorial designs

To perform the sensitivity analysis, a model for each response is required. Because of the complexity of the setup at hand, the modelling of the responses is approximated with regression functions of the form:

$$\eta_M = a_0 + a_1X_1 + \cdots + a_4X_4 + \cdots + a_6X_6 + a_{12}X_1X_2 + \cdots + a_{25}X_2X_5 + \cdots + a_{56}X_5X_6 + a_{123}X_1X_2X_3 + \cdots + a_{456}X_4X_5X_6 \quad (3)$$

$$\eta_e = b_0 + b_1X_1 + \cdots + b_4X_4 + \cdots + b_6X_6 + b_{12}X_1X_2 + \cdots + b_{25}X_2X_5 + \cdots + b_{56}X_5X_6 + b_{123}X_1X_2X_3 + \cdots + b_{456}X_4X_5X_6 \quad (4)$$

where X_1 to X_6 each represent a normalised free factor, and a_0 to a_{456} and b_0 to b_{456} are the parameters of the different models. η_M and η_e respectively model the mutual inductance and the yield of the transformer. In η_M, a_0 is a constant, a_1 to a_6 are called the linear parameters, a_{12} to a_{56} the first-level interaction parameters and a_{123} to a_{456} the second-level interaction parameters. Higher level interactions are neglected due to their small relative value. The same applies to η_e.

The effects of each model are calculated based on the responses, using least square fit. Matrix formulations are used to compute the results. Considering the example of η_M, which is rewritten as:

$$\overrightarrow{\eta_M} = \boldsymbol{X} \cdot \vec{\beta} = \vec{y} - \vec{\varepsilon} \quad (5)$$

where $\boldsymbol{X}$ is an $N \times P$ matrix called the *model matrix*, with N the number of experiments and P the number of effects. Each line represents an experiment, and each column the value of the factor (or combination of factors) for the corresponding experiment. $\vec{\beta}$ is a $P \times 1$ vector containing the effects. The difference between the empirical model $\overrightarrow{\eta_M}$ and the measured responses $\vec{y}$ is called the *residue* $\vec{\varepsilon}$. Of course, after a run of experiments, the unknown is $\vec{\beta}$. Least square fit applied to this system yields:

$$\vec{\beta} = (\boldsymbol{X}^T\boldsymbol{X})^{-1}\boldsymbol{X}^T \cdot \vec{y} \quad (6)$$

Since matrix inversion is necessary to evaluate the effects, the model matrix has to be chosen carefully. In [16], the authors suggest the use of the so-called *full factorial designs at two levels* for such empirical models. For each factor, the extreme acceptable values are taken and normalised such that the value 1 or -1 (often represented respectively by '+' and '-') is assigned to each factor. The factorial design consists in experimenting all possible combinations of 1s and -1s. In the case of 6 free factors, the factorial design contains $N = 2^6 = 64$ experiments (Table 1). In addition to the factorial design, the experimental plan includes the middle point of the space of experiments. For mathematical reasons, the number of experiments should be equal or greater than the number of effects. This condition is fulfilled since the chosen empirical models have 42 effects.

3.3. Evaluation of the Model Parameters

The range of the free factors is given in Table 2, as well as their correspondence with the x_i (which are the non-normalised values of X_i). The normalised value of the model parameters (*effects*) are represented in the bar chart in Fig. 4. The higher an effect is, the more the associated free factor contributes to the response. The two models generate errors smaller than 10% of the maximal values of the model. They could not be used for an optimisation, but are good enough for the identification of important parameters.

As expected, the number of turns of the coils (X_5) is extremely important for the value of the mutual inductance. In the same way, the effect on the flux and flux linkage of the radii of the ferrite plates (X_4) and the coils (X_6) yield to a big effect on the mutual inductance. The size and position of the shielding, although less important, shows to have a rather strong effect. The fact that an effect is positive or negative points out whether a factor tends to increase or decrease an output. However, in such a sensitivity analysis, it only has an informative value.

By analysing the effects of η_e, it appears obvious that the radius of the ferrite plates is essential, as it is for η_M. It must be remembered that the value of the mutual inductance is not an objective, but a functioning constraint. To satisfy this constraint, the radius of the ferrite plates has little freedom. Indeed, when it changes a little, other factors have to be adapted to satisfy the mutual inductance. Even if the effects of the other factors is smaller, they will become the key factors in optimising the transformer, since the largest effect is almost blocked. For these reasons, it is expected to obtain very varied optimal transformers for similar yields.

Also, for the same reasons, it is not possible to exclude one of the parameters from the optimisation. They all have too much influence on the considered outpus.

Table 1. Experimental plan

#	X_1	X_2	X_3	X_4	X_5	X_6
1	-	-	-	-	-	-
2	-	-	-	-	-	+
3	-	-	-	-	+	-
4	-	-	-	-	+	+
5	-	-	-	+	-	-
6	-	-	-	+	-	+
7	-	-	-	+	+	-
8	-	-	+	+	+	+
9	-	-	+	-	-	-
10	-	-	+	-	-	+
11	-	-	+	-	+	-
12	-	-	+	-	+	+
13	-	-	+	+	-	-
14	-	-	+	+	-	+
15	-	-	+	+	+	-
16	-	-	+	+	+	+
17	-	+	-	-	-	-
18	-	+	-	-	-	+
19	-	+	-	-	+	-
20	-	+	-	-	+	+
21	-	+	-	+	-	-
22	-	+	-	+	-	+
23	-	+	-	+	+	-
24	-	+	-	+	+	+
25	-	+	+	-	-	-
26	-	+	+	-	-	+
27	-	+	+	-	+	-
28	-	+	+	-	+	+
29	-	+	+	+	-	-
30	-	+	+	+	-	+
31	-	+	+	+	+	-
32	-	+	+	+	+	+
33	+	-	-	-	-	-
34	+	-	-	-	-	+
35	+	-	-	-	+	-
36	+	-	-	-	+	+
37	+	-	-	+	-	-
38	+	-	-	+	-	+
39	+	-	-	+	+	-
40	+	-	-	+	+	+
41	+	-	+	-	-	-
42	+	-	+	-	-	+
43	+	-	+	-	+	-
44	+	-	+	-	+	+
45	+	-	+	+	-	-
46	+	-	+	+	-	+
47	+	-	+	+	+	-
48	+	-	+	+	+	+
49	+	+	-	-	-	-
50	+	+	-	-	-	+
51	+	+	-	-	+	-
52	+	+	-	-	+	+
53	+	+	-	+	-	-
54	+	+	-	+	-	+
55	+	+	-	+	+	-
56	+	+	-	+	+	+
57	+	+	+	-	-	-
58	+	+	+	-	-	+
59	+	+	+	-	+	-
60	+	+	+	-	+	+
61	+	+	+	+	-	-
62	+	+	+	+	-	+
63	+	+	+	+	+	-
64	+	+	+	+	+	+
65	0	0	0	0	0	0

Table 2. Range of the free factors

Geometric parameter		Min	Max	Factor
Lateral distance between the shielding and the ferrite plate	[mm]	5	50	x_1
Vertical distance between the shielding and the ferrite plate	[mm]	-20	20	x_2
Height of the shielding	[mm]	10	35	x_3
Radius of the ferrite	[mm]	150	350	x_4
Number of turns of the coil	[-]	5	50	x_5
Radius of the coil	[mm]	150	250	x_6

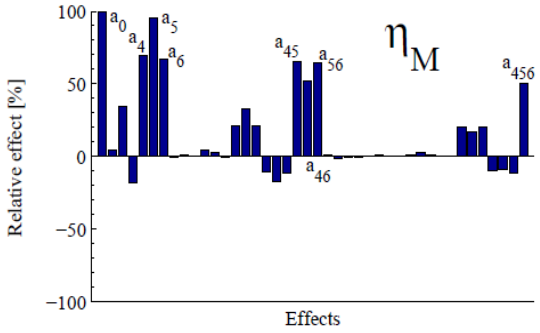

(a)

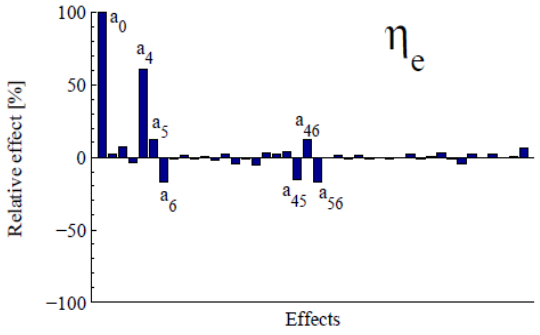

(b)

Fig. 4. Normalised value of the parameters of η_M (a), η_e (b) with most prominent parameters highlighted.

4. Optimisation of the Transformer

The geometry of the transformer is optimized using GA. This is a stochastic global optimisation which is widely used for electromechanical systems [17]–[20]. The two objective functions are to minimise B_{max} and P_{loss} defined in the previous section. A constraint C is defined on the mutual inductance in (7). The target inductance M_{target} is computed according to (2). The inductance M_{mes} is computed via the FEM model.

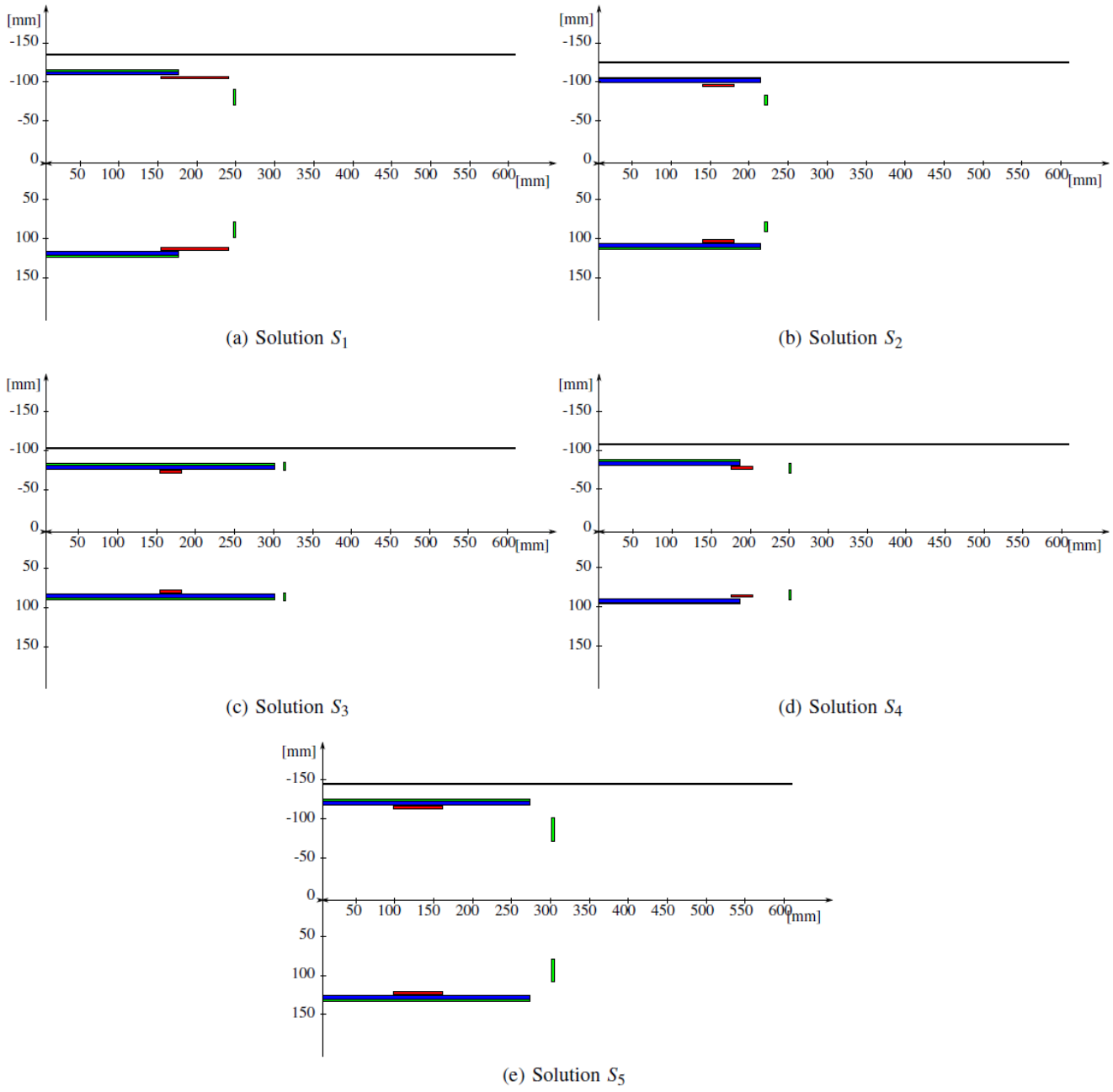

(a) Solution S_1 (b) Solution S_2

(c) Solution S_3 (d) Solution S_4

(e) Solution S_5

Fig. 5. Results of the optimisation

$$C = \begin{cases} 0 \; if \; \dfrac{|M_{target} - M_{mes}|}{M_{target}} \leq 0.1 \\ 100 \; if \; \dfrac{|M_{target} - M_{mes}|}{M_{target}} > 0.1 \end{cases} \quad (7)$$

The results of the optimisation are shown in Fig. 6. And the geometries associated to the five best solutions presented in Fig. 6 (b) are shown in Fig. 5. The normalised values of the factors for these solutions are reported in Table 3.

Some conclusions can be drawn from these results. First of all, the optimisation leads to one optimal point for the two objectives (no Pareto frontier). This means that improving one objective does not necessarily deteriorate the other, which was foreseen with the sensitivity analysis. The

Table 3. Normalised values of the geometric factors

Solution	x_1	x_2	x_3	x_4	x_5	x_6
S_1	-0.96	-0.9	0.33	-0.8	-0.11	0.66
S_2	-1	-0.75	-0.6	-0.45	-0.69	-0.56
S_3	-0.73	0.55	-1	0.42	-0.87	-0.54
S_4	0.82	0.05	-0.84	-0.7	-0.87	-0.06
S_5	0.02	-0.85	0.6	0.15	-0.42	-0.9

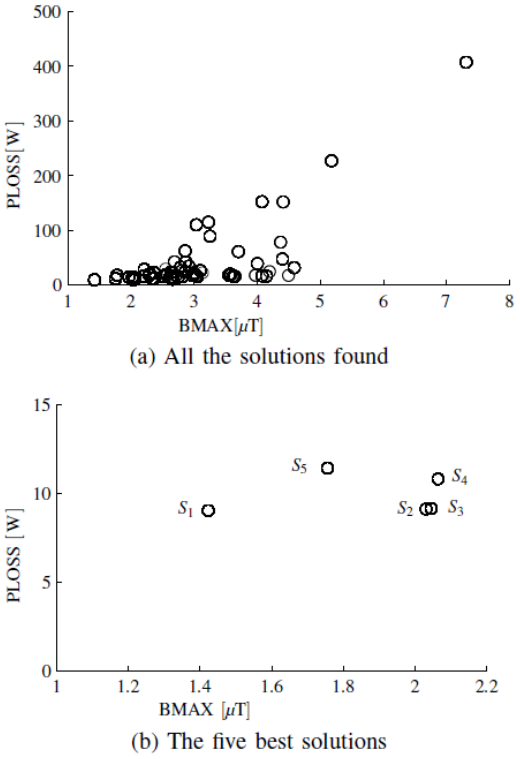

(a) All the solutions found

(b) The five best solutions

Fig. 6. Results of the optimisation

optimised transformers are then of very different shapes, which allows to use other optimisation criteria, such as manufacturing cost, size, weight, or electrical ratings. As expected, the radius of the ferrite is minimal for the solution with the best B_{max} (S_1). In order to satisfy the constraint on the mutual inductance, the radius of the coil is large and the number of turns somewhat high. Another extremely interesting solution is S_3, because the shielding rings are thin and aligned with the ferrite plates. This results in a very thin transformer.

It can also be observed that the boundaries of the experimental plan have been chosen well, since very few of the factors reach the boundary values. Indeed, this means that none of the factors is preventing optimised performance.

5. Conclusion

Throughout this paper, an ICPT system has been studied for power transfer in the range of 500 W. The focus has been made on the magnetic behaviour of the transformer. In order to fulfill European regulation recommendations, the effect of shielding metallic layers on the radiated magnetic field has been taken into account. A sensitivity analysis of the free factors of the transformer has been performed and a global optimisation of the presented topology has been performed in order to reduce the emitted magnetic field nearby the transformer and also minimise the magnetic losses of the shielded transformer. Behavioural tendencies of the ICPT system have been pointed out and various optimal solutions presented.

References

[1] C.-H. Hu, C.-M. Chen, Y.-S. Shiao, T.-J. Chan, and T.-R. Chen, "Development of a universal contactless charger for handheld devices," in Industrial Electronics, 2008. ISIE 2008. IEEE International Symposium on, 30 2008-july 2 2008, pp. 99–104.

[2] P. Meyer, P. Germano, M. Markovic, and Y. Perriard, "Design of a contactless energy transfer system for desktop peripherals," in Energy Conversion Congress and Exposition (ECCE), 2010 IEEE, sept. 2010, pp. 2253–2258.

[3] C. Sonntag, "Contactless energy transfer platform using air-cored planar inductors," Ph.D. dissertation, Eindhoven University of Technology, 2010.

[4] [4] P. Germano, I. Stefanini, and Y. Perriard, "Contactless system dedicated to colic stimulation," in Electrical Machines, 2008. ICEM 2008. 18th International Conference on, sept. 2008, pp. 1–5.

[5] Z. Pantic, S. Bai, and S. Lukic, "Inductively coupled power transfer for continuously powered electric vehicles," in Vehicle Power and Propulsion Conference, 2009. VPPC '09. IEEE, sept. 2009, pp. 1271– 1278.

[6] M. McDonough, P. Shamsi, and B. Fahimi, "Dynamic modeling of icpt considering misalignment and speed of vehicle," in Vehicle Power and Propulsion Conference (VPPC), 2011 IEEE, sept. 2011, pp. 1–6.

[7] I. Stefanini, P. Germano, L. Cardoletti, W. Montella, and Y. Perriard, "Inductive charge system for assembly plant shuttles," in EPE, sept. 2003, pp. 1–5.

[8] F. Nakao, Y. Matsuo, M. Kitaoka, and H. Sakamoto, "Ferrite core couplers for inductive chargers," in Power Conversion Conference, 2002. PCC Osaka 2002. Proceedings of the, vol. 2, 2002, pp. 850– 854 vol.2.

[9] M. Chigira, Y. Nagatsuka, Y. Kaneko, S. Abe, T. Yasuda, and A. Suzuki, "Small-size light-weight transformer with new core structure for contactless electric vehicle power transfer system," in Energy Conversion Congress and Exposition (ECCE), 2011 IEEE, sept. 2011, pp. 260 – 266.

[10] M. Budhia, G. Covic, and J. Boys, "Design and optimization of circular magnetic structures for lumped inductive power transfer systems," Power Electronics, IEEE Transactions on, vol. 26, no. 11, pp. 3096–3108, nov. 2011.

[11] M. Kissin, J. Boys, and G. Covic, "Interphase mutual inductance in polyphase inductive power transfer systems," Industrial Electronics, IEEE Transactions on, vol. 56, no. 7, pp. 2393–2400, 2009.

[12] S. Raabe, G. A. J. Elliott, G. A. Covic, and J. T. Boys, "A quadrature pickup for inductive power transfer systems," in Industrial Electronics and Applications, 2007. ICIEA 2007. 2nd IEEE Conference on, 2007, pp. 68–73.

[13] ICNRP, "Icnirp guidelines for limiting exposure to time-varying electric, magnetic and electromagnetic fields (up to 300 ghz)," 1998.

[14] O. Stielau and G. Covic, "Design of loosely coupled inductive power transfer systems," in Power System Technology, 2000. Proceedings. PowerCon 2000. International Conference on, vol. 1, 2000, pp. 85– 90.

[15] C. Auvigne, P. Germano, D. Ladas, and Y. Perriard, "A dual-topology icpt applied to an electric vehicle battery charger," in Electrical Machines (ICEM), 2012 XXth International Conference on, sept. 2012, pp. 2287–2292.
[16] G. E. P. Box, J. S. Hunter, and W. G. Hunter, Statistics for experimenters. Design, innovation, and discovery. 2nd ed. Wiley Series in Probability and Statistics. Hoboken, NJ: John Wiley & Sons. xvii, 633 p., 2005.
[17] J. Maridor, "Design, optimization and sensorless control of a linear actuator," Ph.D. dissertation, Ecole Polytechnique Federale de Lausanne (EPFL), 2011.
[18] J. Maridor, M. Markovic, Y. Perriard, and D. Ladas, "Optimization design of a linear actuator using a genetic algorithm," in Electric Machines and Drives Conference, 2009. IEMDC '09. IEEE International, may 2009, pp. 1776–1781.
[19] D. Porto, "Design methodology and numerical optimization of ultrasonic transducers for spinal surgery," Ph.D. dissertation, Ecole Polytechnique Federale de Lausanne (EPFL), 2009.
[20] P. Meyer, "Modeling of inductive contactless energy transfer systems," Ph.D. dissertation, Swiss Federal Institute of Technology of Lausanne, 2012.

Romain Besuchet was born in Switzerland, in 1988. He received the M. Sc. In Microengineering from the Swiss Federal Institute of Technology - Lausanne (EPFL) in 2011, after having done his M. Sc. thesis at Zhejiang University, China. He is currently a PhD student in the Integrated Actuator Laboratory at EPFL. His research interests are in the field of miniaturised linear escapement mechanisms and linear actuators.

Christophe Auvigne was born in Ambilly, France, in 1987. He received the M. Sc. in Microengineering from the Swiss Federal Institute of Technology - Lausanne (EPFL) in 2011. He is currently a phd student in the Integrated Actuator Laboratory at EPFL. His research interests are in the field of contactless power transfer and its associated power electronics.

Dan Shi was born in Henan province, China, in 1986. She received the M. Sc. in electrical engineering from the Zhejiang University, Hangzhou, China, in 2012. She is currently a PhD student in the Integrated Actuator Laboratory at the Swiss Federal Institute of Technology - Lausanne (EPFL). Her research interests are in the field of piezoelectric actuators and standing and travelling waves for part feeders.

Christophe Winter was born in Bern, Switzerland, in 1986. He received the M. Sc. in Microengineering from the Swiss Federal Institute of Technology - Lausanne (EPFL) in 2009. He is currently a PhD student in the Integrated Actuator Laboratory at EPFL. His research interests are in the field of piezoelectric haptic actuators (mechanical and electronic drives design) and squeeze film modelling.

Yoan Civet graduated from Grenoble Institute of Technology in France, Swiss FederalInstitute of Technology Lausanne (EPFL) in Switzerland and Politechnico di Torino in Italy with a specialty in Micro and Nanotechnologies for Integrated Systems in 2008, received the Ph.D. degree in Nanoelectronics and Nanotechnologies from the Universit de Grenoble, France, in 2012 for his thesis on MEMS resonators frequency compensation. He then worked on piezoelectric MEMS resonator for haptic devices at TIMA laboratory, Grenoble, France. In 2013, he joined EPFL as Postdoctoral Fellowship. His research activities involve piezoelectric actuators, MEMS, magnetic devices and power transfer.

Yves Perriard was born in Lausanne in 1965. He received the M. Sc. in Microengineering from the Swiss Federal Institute of Technology – Lausanne (EPFL) in 1989 and the PhD. degree in 1992. Senior lecturer from 1998 and professor since 2003, he is currently director of the Integrated Actuator Laboratory at EPFL. His research interests are in the field of new actuator design and associated electronic devices.